Electronic Supplementary Material (ESI) for Organic & Biomolecular Chemistry.
This journal is © The Royal Society of Chemistry 2019

Selective binding of nucleosides to gapped DNA duplex revealed by orientation and distance dependence of FRET

Hiromu Kashida*, Yuta Kokubo, Koki Makino and Hiroyuki Asanuma*

kashida@chembio.nagoya-u.ac.jp (H.K.); asanuma@chembio.nagoya-u.ac.jp (H.A.)

Table of Contents

General

Oligonucleotides

All conventional phosphoramidite monomers, CPG columns, reagents for DNA synthesis, and Poly-Pak II cartridges were purchased from Glen Research. Other reagents for the synthesis of phosphoramidite monomers were purchased from Tokyo Chemical Industry, Wako, and Aldrich. Native oligodeoxyribonucleotides were purchased from Integrated DNA Technologies.

Dye-conjugated oligonucleotides were synthesized on an automated DNA synthesizer (H-8-SE, Gene World) as we reported previously.[1] Oligonucleotides were purified by reversed-phase HPLC and characterized by MALDI-TOF MS (Autoflex II, Bruker Daltonics) and HPLC.

The MALDI-TOFMS data for the modified DNA were as follows: **P1-T**: Obsd. 10214 (Calcd. for [**P1-T**+H^+]: 10220). **P2-T**: Obsd. 10214 (Calcd. for [**P2-T**+H^+]: 10220). **P3-T**: Obsd. 10214 (Calcd. for [**P3-T**+H^+]: 10220). **P4-T**: Obsd. 10217 (Calcd. for [**P4-T**+H^+]: 10220). **P2-C**: Obsd. 10203 (Calcd. for [**P2-C**+H^+]: 10205). **P2-G**: Obsd. 10238 (Calcd. for [**P2-G**+H^+]: 10245). **P2-A**: Obsd. 10225 (Calcd. for [**P2-A**+H^+]: 10229). **P2-TT**: Obsd. 10205 (Calcd. for [**P2-TT**+H^+]: 10211). **P2-CT**: Obsd. 10191 (Calcd. for [**P2-CT**+H^+]: 10196). **E1**: Obsd. 4130 (Calcd. for [**E1**+H^+]: 4130). **E2**: Obsd. 4130 (Calcd. for [**E2**+H^+]: 4130). **E3**: Obsd. 4130 (Calcd. for [**E3**+H^+]: 4130). **E4**: Obsd. 4129 (Calcd. for [**E4**+H^+]: 4130).

Fluorescence measurements with nucleosides

Fluorescence spectra were measured on JASCO model FP-8500. The excitation wavelength was 345 nm. Band widths were 5 nm for excitation and emission. Before measurements, sample solutions containing DNA duplex were heated at 80 ºC, then slowly cooled down to 20 ºC at a rate of 1 ºC min^{-1}. Samples with various concentrations of nucleosides were prepared and measured separately. Their emission intensities were normalized by the emission intensity at 80 ºC. Emission spectra shown in this paper were measured at 20 ºC unless otherwise noted. Sample solutions contained 500 mM NaCl, 10 mM phosphate buffer, pH 7.0. Concentrations of oligonucleotides were 0.2 μM for those tethering pyrene (**P1-T** to **P4-T**, **P2-C**, **P2-G**, **P2-A**, **P2-TT** and **P2-CT**), 0.4 μM for those tethering perylene (**E1** to **E4** and **N3**) and 0.6 μM for native strands (**N1** and **N2**).

Circular dichroism (CD) measurement

CD spectra were measured on a JASCO model J-820 equipped with programmed temperature controllers using 10-mm quartz cells. Sample solutions containing DNA were heated at 80 ºC for 4 min, then slowly cooled down to 20 ºC at a rate of 1.0 ºC min^{-1}. Spectra were measured at 10 ºC intervals. CD spectra shown in this paper were measured at 20 ºC. Sample solutions contained 500 mM NaCl, 10 mM phosphate buffer (pH 7.0) and 1.0 μM DNA.

Experimental calculation of FRET efficiency

FRET efficiency (Φ_T) was experimentally determined from the decrease in donor emission:

$$\Phi_T = 1 - I_{DA} / I_D \quad (1)$$

where I_{DA} is emission intensity of a duplex containing a donor and an acceptor at 405 nm, and I_D is that of donor-only duplex at 405 nm. For the determination of FRET efficiencies, fluorescence spectra were measured over the range from 80 to 20 ºC at 10 ºC intervals with 4-minute incubations after each temperature change. Emission intensities were measured at 20 ˚C. Sample solutions contained 500 mM NaCl, 10 mM phosphate buffer, pH 7.0. Concentrations of oligonucleotides were 0.2 μM for those tethering pyrene (**P1-T** to **P4-T**), 0.4 μM for those tethering perylene (**E1** to **E4**, **N3** and **N4**) and 0.6 μM for native strands (**N1** and **N2**). Each emission intensity was normalized at the intensity at 80 ˚C in order to eliminate the effects of concentration errors. Error bars of FRET efficiencies show standard deviations of three independent experiments.

Determination of binding constants

Binding constants of nucleosides (N) to duplex with a 1-nt gap (G) were analysed assuming the following equilibrium:

$$\mathrm{G} + \mathrm{N} \underset{K_\mathrm{d}}{\rightleftharpoons} \mathrm{G-N} \quad (2)$$

where the complex is G-N. We plotted the ratio of pyrene emission intensity to perylene intensity (I_{405}/I_{510}) against the concentration of the nucleoside. Since excess amount of nucleoside was used for fluorescence measurements, the I_{405}/I_{510} can be calculated from the following equations:

$$\frac{I_{405}}{I_{510}} = \frac{I_{G,405}\alpha + I_{G-N,405}\beta}{I_{G,510}\alpha + I_{G-N,510}\beta} \quad (3)$$

$$\alpha = \frac{K_d}{K_d + [N]_0} \quad (4)$$

$$\beta = \frac{[N]_0}{K_d + [N]_0} \quad (5)$$

where $I_{G\text{-}N}$ and I_G are emission intensities of G-N and G, respectively, $[N]_0$ is the total concentration of nucleoside, and α and β are fractions of G and G-N, respectively. Subscripts of $I_{G\text{-}N}$ and I_G indicate monitored wavelengths. $I_{G,405}$ and $I_{G,510}$ were directly determined from emission intensities of gapped DNA at 405 and 510 nm, respectively. $I_{G\text{-}N,405}$ and $I_{G\text{-}N,510}$ were determined by using plots of pyrene and perylene intensities against nucleoside concentration. K_d was determined by fitting the experimentally obtained I_{405}/I_{510} ratio to the ratio calculated using equations (3) to (5). Optimization of parameters was performed by least-squares method using Solver tool in Microsoft Excel.

Binding of nucleosides to the duplex with a 2-nt gap (**TT-Gap**) was analysed by using a similar method using the following equation:

$$\mathrm{G} + 2\mathrm{N} \underset{K_{\mathrm{d1}}}{\overset{\longrightarrow}{\longleftarrow}} \mathrm{G} - \mathrm{N} + \mathrm{N} \underset{K_{\mathrm{d2}}}{\overset{\longrightarrow}{\longleftarrow}} \mathrm{G} - 2\mathrm{N} \tag{6}$$

where G-2N is the complex of gapped duplex with two molecules of nucleoside. K_{d1} and K_{d2} are dissociation constants of the first and second equilibrium, respectively. The I_{405}/I_{510} ratio can be calculated from the following equations:

$$\frac{I_{405}}{I_{510}} = \frac{I_{G,405}\alpha + I_{G-N,405}\beta + I_{G-2N,405}\gamma}{I_{G,510}\alpha + I_{G-N,510}\beta + I_{G-2N,510}\gamma} \tag{7}$$

$$\alpha = \frac{K_{d1}K_{d2}}{K_{d1}K_{d2} + [N]_0 K_{d2} + {[N]_0}^2} \tag{8}$$

$$\beta = \frac{[N]_0 K_{d2}}{K_{d1}K_{d2} + [N]_0 K_{d2} + {[N]_0}^2} \tag{9}$$

$$\gamma = \frac{{[N]_0}^2}{K_{d1}K_{d2} + [N]_0 K_{d2} + {[N]_0}^2} \tag{10}$$

where $I_{G\text{-}2N}$, $I_{G\text{-}N}$, and I_G are emission intensities of the G-2N, G-N, and G, respectively, $[N]_0$ is the total concentration of nucleoside, and α, β, and γ are fractions of G, G-N, and G-2N, respectively. Values of I_{405} and I_{510} of G were directly determined from emission intensities G at 405 and 510 nm, respectively. Those of G-N were estimated from fluorescence intensities of **T-Gap**. I_{405} and I_{510} of G-2N were determined using plots of pyrene and perylene intensities versus nucleoside concentration. K_{d1} and K_{d2} were determined by fitting experimentally obtained I_{405}/I_{510} ratios to the ratios calculated by using equations (7) to (10). Optimization of parameters was performed using the least-squares method with the Solver tool in Microsoft Excel.

Theoretical calculation of energy transfer efficiencies based on Förster theory

Energy transfer efficiency was calculated from the following equations:

$$\Phi_T = \frac{1}{1 + (\frac{R}{R_0})^6} \tag{11}$$

$$R_0 = 0.2108[J(\lambda)\kappa^2 n^{-4}\Phi_D]^{1/6} \tag{12}$$

where R is the distance between donor and acceptor, R_0 is a Förster radius (the distance where Φ_T equals 0.5), $J(\lambda)$ is the integral of spectral overlap between absorption and emission of perylene, n is a refractive index (which is typically assumed to be 1.4 for biomolecules), and Φ_D is a quantum yield of perylene. When dyes are located in parallel planes, the orientation factor, κ^2, can be calculated by using the angle between transition dipoles of dyes (θ_T):

$$\kappa^2 = cos^2\theta_T \tag{13}$$

Theoretical transfer efficiency can be calculated from the distance and angle between two chromophores. Typical rise and typical twist angle of B-form duplex, 3.6 Å per base pair and 32 º per base pair, respectively, were used to calculate the distance and the angle between dyes. We used an angle of 42º between dyes angles, which was reported previously.[2] Consequently, the angle between dyes (θ_T) was calculated from the following equation:

$$\theta_T = 32^\circ \times (n-1) + 42^\circ \quad (14)$$

where *n* is the number of base pairs between dyes.

We also calculated a theoretical curve with averaged dye orientation by using κ^2 of 2/3.

Isothermal titration calorimetry

Calorimetric measurements were carried out using MicroCal iTC200 in 500 mM NaCl, 10 mM phosphate buffer (pH 7.0). The experiment was conducted by adding nucleoside every 3 min into the solution of DNA maintained at 25 ºC. Heats of dilution were measured in blank titrations by injecting nucleoside into the buffer and were subtracted from the binding heats. Thermodynamic parameters were determined by nonlinear least-squares methods using routines included in the Origin software package (MicroCal, version 7.0).

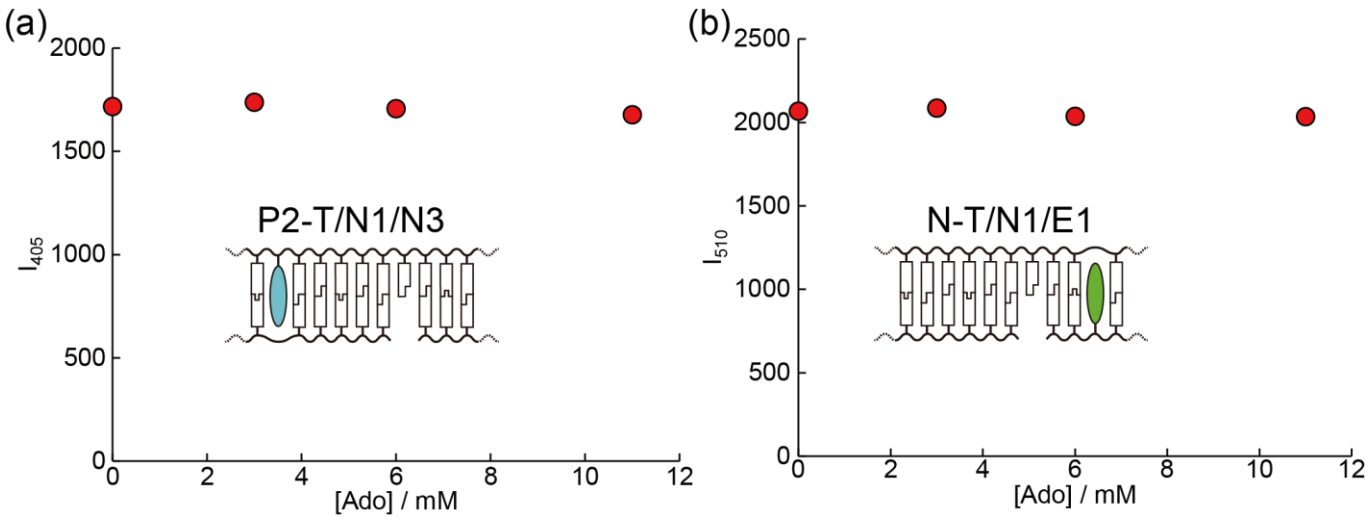

Fig. S1. Effects of the binding of adenosine on the emission of (a) pyrene or (b) perylene at 20 ºC. Excitation and emission wavelengths are 345 and 405 nm for (a), or 425 and 510 nm for (b). Sequences are shown below.

P2-T	ATCAGTATGTATGT**P**ATGTA**T**TC-ACCGTAGTCA	(5′→3′)
N1/N3	TAGTCATACATACA-TACAT□AGTGGCATCAGT	(3′←5′)
N-T	ATCAGTATGTATGTATGTA**T**TC-ACCGTAGTCA	(5′→3′)
N1/E1	TAGTCATACATACATACAT□AG**E**TGGCATCAGT	(3′←5′)

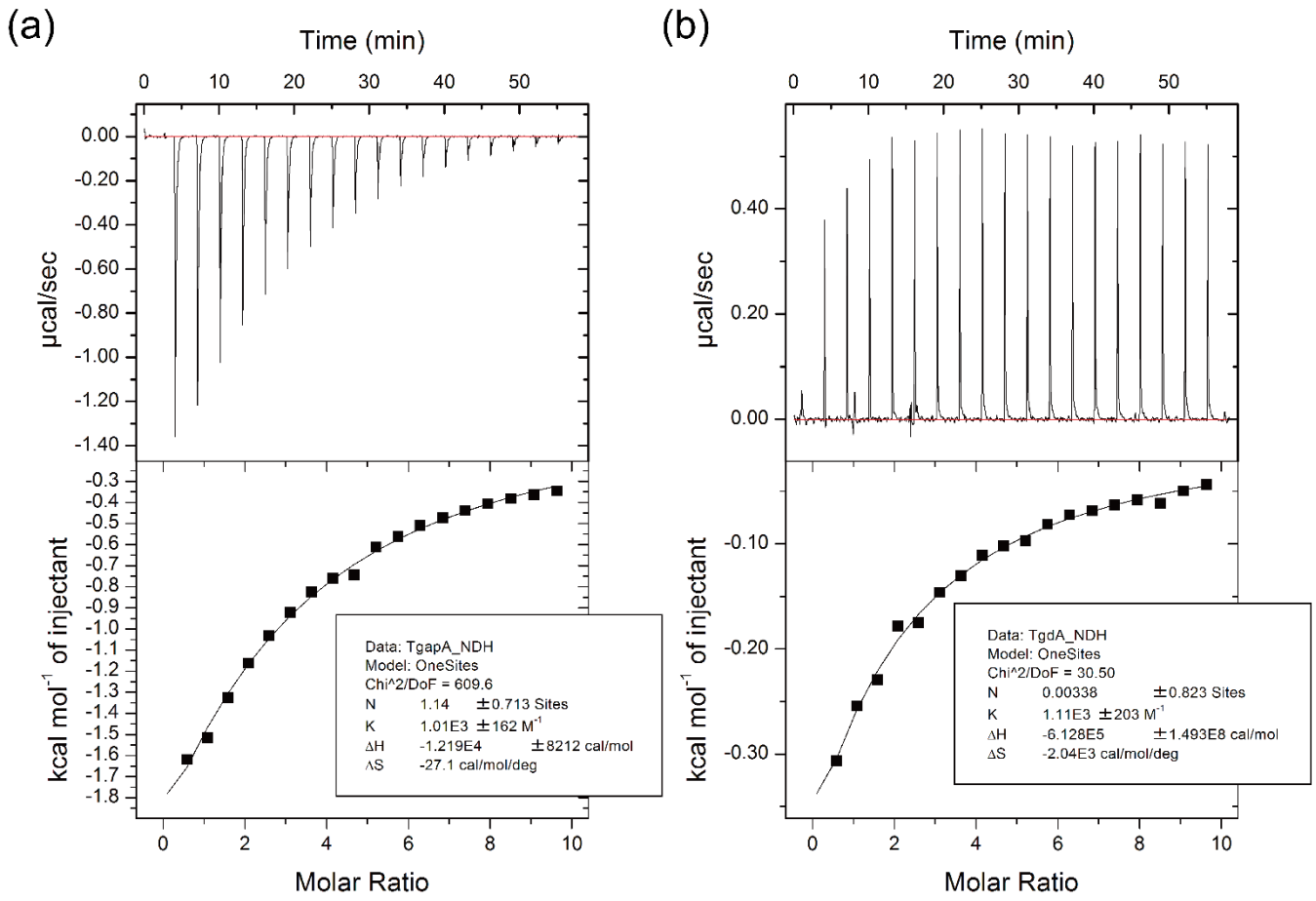

Fig. S2. Plots of heat release as a function of molar ratio of adenosine to duplex for (a) **Native T-Gap** and (b) **T-Gap**.

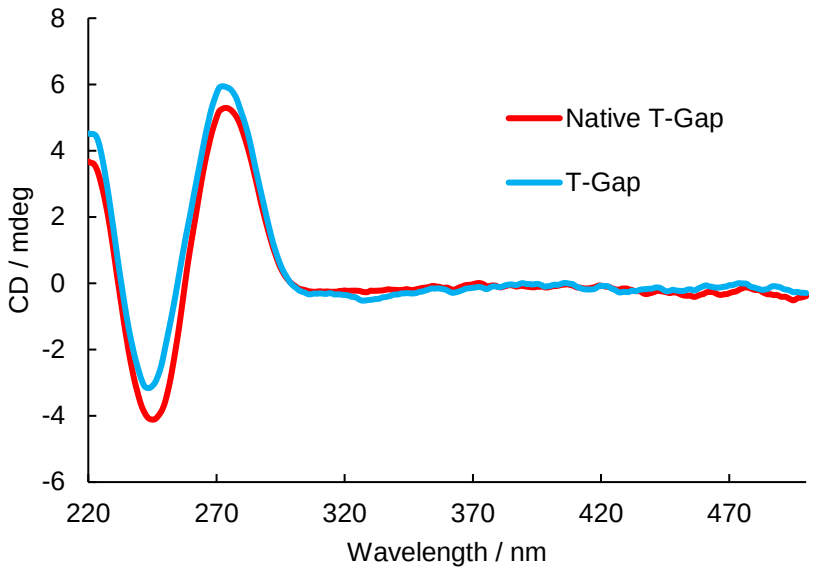

Fig. S3. CD spectra of **T-Gap** and **Native T-Gap** measured at 20 ºC.

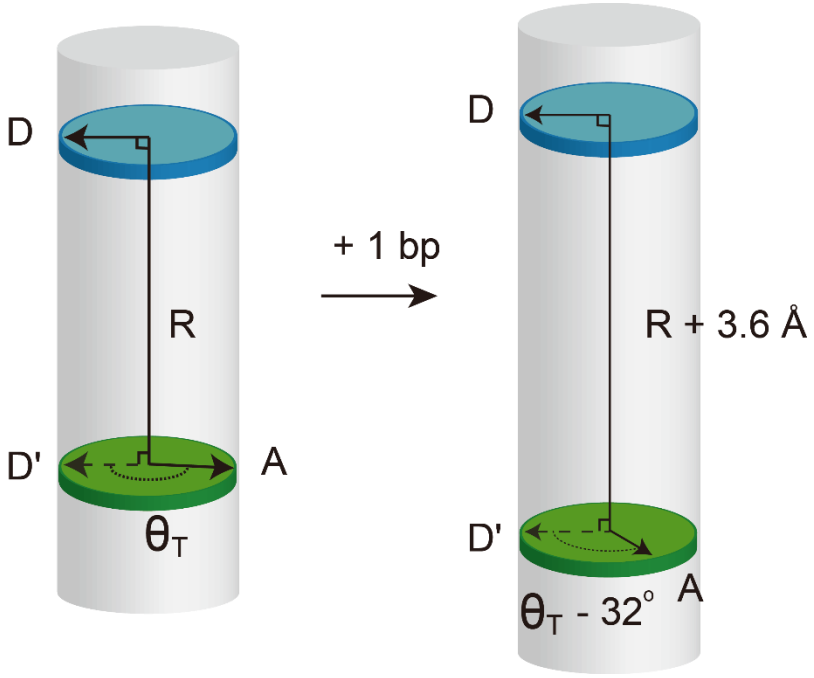

Fig. S4. Cylinder model used to calculate theoretical FRET efficiency.

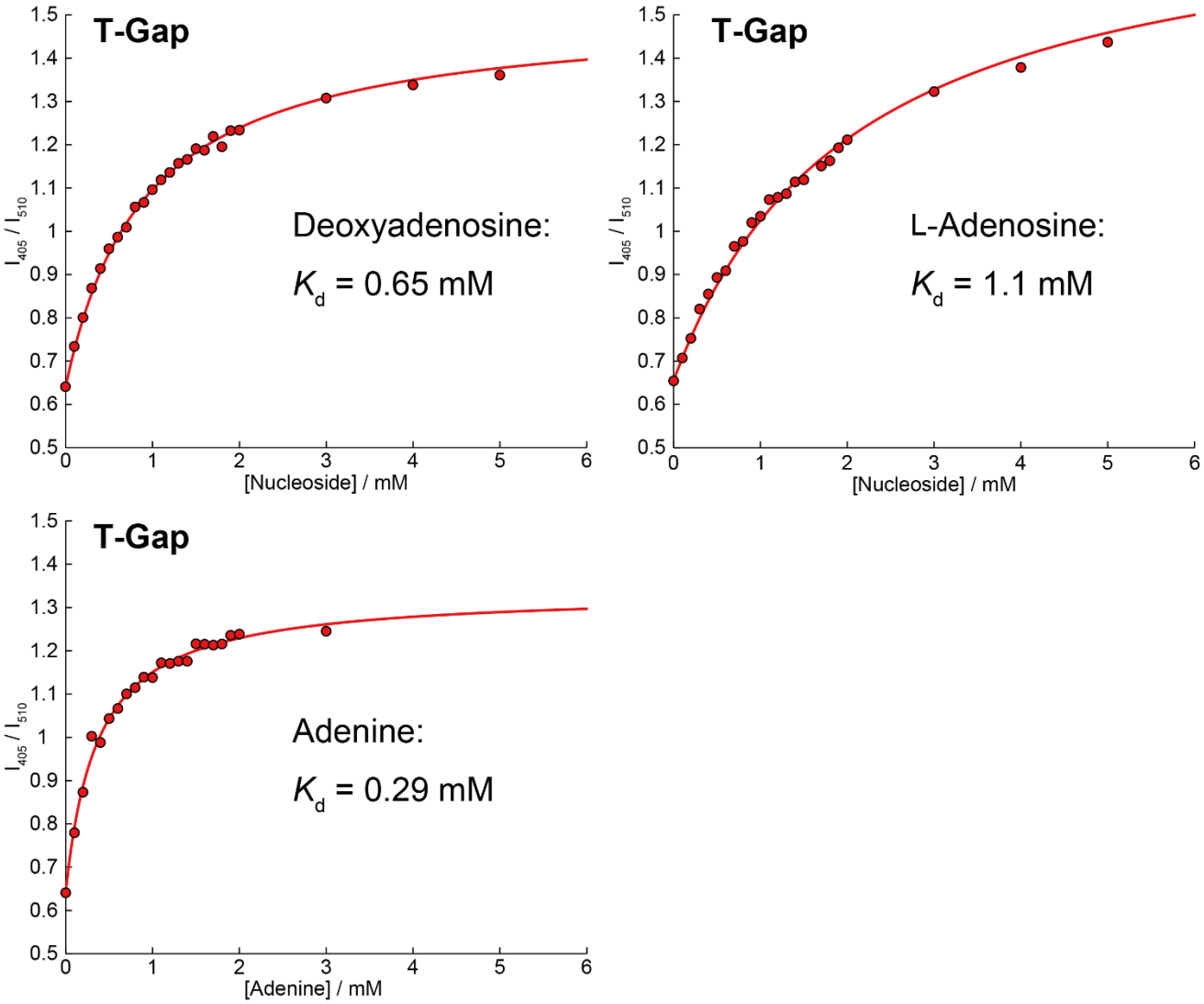

Fig. S5. Plots of I_{405}/I_{510} of **T-Gap** versus concentration of deoxyadenosine, L-adenosine, and adenine.

Table S1. Sequences of gapped and nicked duplexes used in this study.

Duplex Name	Strand Names	Sequences	Orientation
T-Gap	P2-T	ATCAGTATGTATGT**P**ATGTA**T**TC-ACCGTAGTCA	(5′→3′)
	N1/E1	TAGTCATACATACA-TACAT□AG**E**TGGCATCAGT	(3′←5′)
C-Gap	P2-C	ATCAGTATGTATGT**P**ATGTA**C**TC-ACCGTAGTCA	(5′→3′)
	N1/E1	TAGTCATACATACA-TACAT□AG**E**TGGCATCAGT	(3′←5′)
G-Gap	P2-G	ATCAGTATGTATGT**P**ATGTA**G**TC-ACCGTAGTCA	(5′→3′)
	N1/E1	TAGTCATACATACA-TACAT□AG**E**TGGCATCAGT	(3′←5′)
A-Gap	P2-A	ATCAGTATGTATGT**P**ATGTA**A**TC-ACCGTAGTCA	(5′→3′)
	N1/E1	TAGTCATACATACA-TACAT□AG**E**TGGCATCAGT	(3′←5′)
TT-Gap	P2-TT	ATCAGTATGTATGT**P**ATGT**TT**TC-ACCGTAGTCA	(5′→3′)
	N1/E1	TAGTCATACATACA-TACA□□AG**E**TGGCATCAGT	(3′←5′)
CT-Gap	P2-CT	ATCAGTATGTATGT**P**ATGT**CT**TC-ACCGTAGTCA	(5′→3′)
	N1/E1	TAGTCATACATACA-TACA□□AG**E**TGGCATCAGT	(3′←5′)
Nick	P2-T	ATCAGTATGTATGT**P**ATGTATTC-ACCGTAGTCA	(5′→3′)
	N2/E1	TAGTCATACATACA-TACATAAG**E**TGGCATCAGT	(3′←5′)
Native T-Gap	N-T	ATCAGTATGTATGTATGTATTCACCGTAGTCA	(5′→3′)
	N1/N4	TAGTCATACATACATACAT□AGTGGCATCAGT	(3′←5′)

Table S2. FRET efficiencies of duplexes with 1-nt gaps with and without adenosine.

Distance	Sequence			Φ_T	
				w/o adenosine	with 3 mM adenosine
4 nt	P1-T N1/E1	ATCAGTATGTATGTATGT**P**A**T**TC-ACCGTAGTCA TAGTCATACATACATACA-T□AG**E**TGGCATCAGT	(5′→3′) (3′←5′)	0.94	0.96
5 nt	P1-T N1/E2	ATCAGTATGTATGTATGT**P**A**T**TCA-CCGTAGTCA TAGTCATACATACATACA-T□AGT**E**GGCATCAGT	(5′→3′) (3′←5′)	0.93	0.96
6 nt	P1-T N1/E3	ATCAGTATGTATGTATGT**P**A**T**TCAC-CGTAGTCA TAGTCATACATACATACA-T□AGTG**E**GCATCAGT	(5′→3′) (3′←5′)	0.92	0.92
7 nt	P1-T N1/E4	ATCAGTATGTATGTATGT**P**A**T**TCACC-GTAGTCA TAGTCATACATACATACA-T□AGTGG**E**CATCAGT	(5′→3′) (3′←5′)	0.86	0.80
8 nt (**T-Gap**)	P2-T N1/E1	ATCAGTATGTATGT**P**ATGTA**T**TC-ACCGTAGTCA TAGTCATACATACA-TACAT□AG**E**TGGCATCAGT	(5′→3′) (3′←5′)	0.66	0.54
9 nt	P2-T N1/E2	ATCAGTATGTATGT**P**ATGTA**T**TCA-CCGTAGTCA TAGTCATACATACA-TACAT□AGT**E**GGCATCAGT	(5′→3′) (3′←5′)	0.49	0.46
10 nt	P2-T N1/E3	ATCAGTATGTATGT**P**ATGTA**T**TCAC-CGTAGTCA TAGTCATACATACA-TACAT□AGTG**E**GCATCAGT	(5′→3′) (3′←5′)	0.47	0.52
11 nt	P2-T N1/E4	ATCAGTATGTATGT**P**ATGTA**T**TCACC-GTAGTCA TAGTCATACATACA-TACAT□AGTGG**E**CATCAGT	(5′→3′) (3′←5′)	0.46	0.46
12 nt	P3-T N1/E1	ATCAGTATGT**P**ATGTATGTA**T**TC-ACCGTAGTCA TAGTCATACA-TACATACAT□AG**E**TGGCATCAGT	(5′→3′) (3′←5′)	0.38	0.30
13 nt	P3-T N1/E2	ATCAGTATGT**P**ATGTATGTA**T**TCA-CCGTAGTCA TAGTCATACA-TACATACAT□AGT**E**GGCATCAGT	(5′→3′) (3′←5′)	0.23	0.14
14 nt	P3-T N1/E3	ATCAGTATGT**P**ATGTATGTA**T**TCAC-CGTAGTCA TAGTCATACA-TACATACAT□AGTG**E**GCATCAGT	(5′→3′) (3′←5′)	0.13	0.07
15 nt	P3-T N1/E4	ATCAGTATGT**P**ATGTATGTA**T**TCACC-GTAGTCA TAGTCATACA-TACATACAT□AGTGG**E**CATCAGT	(5′→3′) (3′←5′)	0.16	0.12
16 nt	P4-T N1/E1	ATCAGT**P**ATGTATGTATGTA**T**TC-ACCGTAGTCA TAGTCA-TACATACATACAT□AG**E**TGGCATCAGT	(5′→3′) (3′←5′)	0.09	0.11
17 nt	P4-T N1/E2	ATCAGT**P**ATGTATGTATGTA**T**TCA-CCGTAGTCA TAGTCA-TACATACATACAT□AGT**E**GGCATCAGT	(5′→3′) (3′←5′)	0.09	0.08
18 nt	P4-T N1/E3	ATCAGT**P**ATGTATGTATGTA**T**TCAC-CGTAGTCA TAGTCA-TACATACATACAT□AGTG**E**GCATCAGT	(5′→3′) (3′←5′)	0.07	0.03
19 nt	P4-T N1/E4	ATCAGT**P**ATGTATGTATGTA**T**TCACC-GTAGTCA TAGTCA-TACATACATACAT□AGTGG**E**CATCAGT	(5′→3′) (3′←5′)	0.05	0.02
Control	P1-T N1/N3	ATCAGTATGTATGTATGT**P**A**T**TCACCGTAGTCA TAGTCATACATACATACA-T□AGTGGCATCAGT	(5′→3′) (3′←5′)	-	-
Control	P2-T N1/N3	ATCAGTATGTATGT**P**ATGTA**T**TCACCGTAGTCA TAGTCATACATACA-TACAT□AGTGGCATCAGT	(5′→3′) (3′←5′)	-	-
Control	P3-T N1/N3	ATCAGTATGT**P**ATGTATGTA**T**TCACCGTAGTCA TAGTCATACA-TACATACAT□AGTGGCATCAGT	(5′→3′) (3′←5′)	-	-
Control	P4-T N1/N3	ATCAGT**P**ATGTATGTATGTA**T**TCACCGTAGTCA TAGTCA-TACATACATACAT□AGTGGCATCAGT	(5′→3′) (3′←5′)	-	-

Table S3. FRET efficiencies of nicked duplexes.

Distance	Sequence			Φ_T
4 nt	P1-T	ATCAGTATGTATGTATGT**P**ATTC-ACCGTAGTCA	(5′→3′)	0.97
	N2/E1	TAGTCATACATACATACA-TAAG**E**TGGCATCAGT	(3′←5′)	
5 nt	P1-T	ATCAGTATGTATGTATGT**P**ATTCA-CCGTAGTCA	(5′→3′)	0.97
	N2/E2	TAGTCATACATACATACA-TAAGT**E**GGCATCAGT	(3′←5′)	
6 nt	P1-T	ATCAGTATGTATGTATGT**P**ATTCAC-CGTAGTCA	(5′→3′)	0.93
	N2/E3	TAGTCATACATACATACA-TAAGTG**E**GCATCAGT	(3′←5′)	
7 nt	P1-T	ATCAGTATGTATGTATGT**P**ATTCACC-GTAGTCA	(5′→3′)	0.80
	N2/E4	TAGTCATACATACATACA-TAAGTGG**E**CATCAGT	(3′←5′)	
8 nt (**Nick**)	P2-T	ATCAGTATGTATGT**P**ATGTATTC-ACCGTAGTCA	(5′→3′)	0.43
	N2/E1	TAGTCATACATACA-TACATAAG**E**TGGCATCAGT	(3′←5′)	
9 nt	P2-T	ATCAGTATGTATGT**P**ATGTATTCA-CCGTAGTCA	(5′→3′)	0.50
	N2/E2	TAGTCATACATACA-TACATAAGT**E**GGCATCAGT	(3′←5′)	
10 nt	P2-T	ATCAGTATGTATGT**P**ATGTATTCAC-CGTAGTCA	(5′→3′)	0.57
	N2/E3	TAGTCATACATACA-TACATAAGTG**E**GCATCAGT	(3′←5′)	
11 nt	P2-T	ATCAGTATGTATGT**P**ATGTATTCACC-GTAGTCA	(5′→3′)	0.48
	N2/E4	TAGTCATACATACA-TACATAAGTGG**E**CATCAGT	(3′←5′)	
12 nt	P3-T	ATCAGTATGT**P**ATGTATGTATTC-ACCGTAGTCA	(5′→3′)	0.25
	N2/E1	TAGTCATACA-TACATACATAAG**E**TGGCATCAGT	(3′←5′)	
13 nt	P3-T	ATCAGTATGT**P**ATGTATGTATTCA-CCGTAGTCA	(5′→3′)	0.07
	N2/E2	TAGTCATACA-TACATACATAAGT**E**GGCATCAGT	(3′←5′)	
14 nt	P3-T	ATCAGTATGT**P**ATGTATGTATTCAC-CGTAGTCA	(5′→3′)	0.05
	N2/E3	TAGTCATACA-TACATACATAAGTG**E**GCATCAGT	(3′←5′)	
15 nt	P3-T	ATCAGTATGT**P**ATGTATGTATTCACC-GTAGTCA	(5′→3′)	0.11
	N2/E4	TAGTCATACA-TACATACATAAGTGG**E**CATCAGT	(3′←5′)	
16 nt	P4-T	ATCAGT**P**ATGTATGTATGTATTC-ACCGTAGTCA	(5′→3′)	0.11
	N2/E1	TAGTCA-TACATACATACATAAG**E**TGGCATCAGT	(3′←5′)	
17 nt	P4-T	ATCAGT**P**ATGTATGTATGTATTCA-CCGTAGTCA	(5′→3′)	0.06
	N2/E2	TAGTCA-TACATACATACATAAGT**E**GGCATCAGT	(3′←5′)	
18 nt	P4-T	ATCAGT**P**ATGTATGTATGTATTCAC-CGTAGTCA	(5′→3′)	0.01
	N2/E3	TAGTCA-TACATACATACATAAGTG**E**GCATCAGT	(3′←5′)	
19 nt	P4-T	ATCAGT**P**ATGTATGTATGTATTCACC-GTAGTCA	(5′→3′)	0.01
	N2/E4	TAGTCA-TACATACATACATAAGTGG**E**CATCAGT	(3′←5′)	
Control	P1-T	ATCAGTATGTATGTATGT**P**ATTCACCGTAGTCA	(5′→3′)	-
	N2/N3	TAGTCATACATACATACA-TAAGTGGCATCAGT	(3′←5′)	
Control	P2-T	ATCAGTATGTATGT**P**ATGTATTCACCGTAGTCA	(5′→3′)	-
	N2/N3	TAGTCATACATACA-TACATAAGTGGCATCAGT	(3′←5′)	
Control	P3-T	ATCAGTATGT**P**ATGTATGTATTCACCGTAGTCA	(5′→3′)	-
	N2/N3	TAGTCATACA-TACATACATAAGTGGCATCAGT	(3′←5′)	
Control	P4-T	ATCAGT**P**ATGTATGTATGTATTCACCGTAGTCA	(5′→3′)	-
	N2/N3	TAGTCA-TACATACATACATAAGTGGCATCAGT	(3′←5′)	

Supplementary References

[1] a) H. Asanuma, M. Akahane, N. Kondo, T. Osawa, T. Kato, H. Kashida, *Chem. Sci.* **2012**, *3*, 3165-3169; b) T. Doi, T. Sakakibara, H. Kashida, Y. Araki, T. Wada, H. Asanuma, *Chem. Eur. J.* **2015**, *21*, 15974-15980.

[2] H. Kashida, A. Kurihara, H. Kawai, H. Asanuma, *Nucleic Acids Res.* **2017**, *45*, e105-e105.